9.8

SCREEN-HEIGHT OBSERVATIONS ASSIMILATED IN AN EVOLVING 1-D PBL WITH AN ENSEMBLE KALMAN FILTER

Joshua P. Hacker* **and Chris Snyder**
The National Center for Atmospheric Research†, Boulder, CO

1. Introduction

Surface-layer in-situ observations represent a rich, accurate, and often dense data source, but they are generally under-utilized in current operational data assimilation (DA) systems because of the complex interactions between the surface and the atmosphere aloft. In addition, when precipitation is absent and the winds are light, limiting the utility of radar, surface (screen-height) observations are often the only reliable data source in the PBL. Representing the structure of the planetary boundary layer (PBL) accurately in a mesoscale NWP model initialization could lead to improved short-range forecasts of convective outbreaks, slope flows, and frontal propagation. When a mesoscale NWP model is used as a tool to generate 3-D datasets for process studies, an accurate representation of the PBL would also be valuable.

Studies have shown that a Newtonian relaxation (nudging) approach can often lead to a better representation of the PBL (e.g. Stauffer et al. 1991; Miller and Benjamin 1992; Fast 1995; Leidner et al. 2001). These results rely on imposing an assumed PBL structure that matches both the observation and the free atmosphere aloft. The approach accounts for the bulk properties of the PBL under different stability conditions. More sophisticated profile-matching techniques have been successful when combined with an incremental update DA system (Ruggiero et al. 1996). To our knowledge, neither PBL dynamics nor background covariance information has been explicitly included in a PBL initialization scheme.

This study uses an ensemble Kalman filter (ENKF; Anderson and Anderson 1999) to simulate a screen-height observation DA in an evolving PBL over several days. The goal is to establish the capabilities of the ENKF and lay the groundwork for extending the method to parameter estimation in 3-D. The ENKF has the advantage that background error covariances are time-dependent and can be highly anisotropic. In cases where the forecast screen-height temperature is strongly correlated with the structure of the rest of the PBL, the ENKF approach should rapidly correct the entire PBL. High correlation between screen-height temperatures and the structure of the PBL is expected under convective conditions, but experimentation is necessary to determine whether the ENKF maintains its effectiveness over a wide range of conditions.

**Corresponding author address:* Joshua Hacker, National Center for Atmospheric Research, P.O. Box 3000, Boulder, CO 80307. Email: hacker@ucar.edu

†The National Center for Atmospheric Research is sponsored by the National Science Foundation

2. Experiment description

To create a simple framework for PBL data assimilation experiments, a perfect model is assumed. We have adopted a PBL/land-surface parameterization scheme as the model — chosen because it contains the minimum physics consistent with a current NWP model and is simple enough to elucidate the interaction between the ENKF and the model state. A model climatology is created that represents the "truth". Observations are sampled from the "truth", assimilated into an ensemble of perturbed states via the ENKF, and compared to a simple nudging scheme and an ensemble running without assimilation. Single-layer temperature observations are assimilated to assess the ability of the ENKF to spread the observations through the appropriate depth.

The so-called MRF PBL scheme (Troen and Mahrt 1986; Hong and Pan 1996) is extracted from the Weather Research and Forecasting (WRF) model so that it can be run in 1-D with controlled forcing but no external physics (such as pressure gradients, latent heating, and cloud and radiation feedback). A 5-layer slab soil model and a surface-layer similarity scheme are coupled with the PBL diffusion scheme to create a stand-alone system, which is forced with a diurnal solar radiation cycle. An Earth location of 100°W, 35°N and a 0.2 cloud-cover fraction are assumed to parameterize down-welling solar radiation. The Stefan-Boltzmann law applied to the lowest model level gives down-welling long-wave radiation.

A year-long integration is used to generate a model cli-

matology that defines a range of possible model states. The solar declination angle changes with the Julian day, creating a seasonal cycle upon which the diurnal cycle is superimposed. The solution relaxes toward a constant vertical wind shear of 5.0 m s^{-1} km^{-1} on a 1-day time scale. Surface parameters are chosen to match a summer agricultural surface as assumed in the slab soil model: the albedo (α) is 0.17, the surface roughness (z_0) is 0.15 m, emissivity (ε) is 0.92, and thermal inertia is 0.04 Cal cm^{-2} K^{-1} $s^{-1/2}$. Surface moisture content and potential evaporation is included in one static "moisture availability" parameter, which is specified as 0.3.

Because full physics are excluded and external feedback is ignored, the only nonlinearities in the system exist in the solution to the diffusion equation and therefore nonlinear error growth is not expected. This is consistent with the assertion that the state of the PBL is largely controlled by surface fluxes and the temperature jump between the PBL and the free atmosphere aloft (Deardorff 1972). Two integrations, initialized with similar ratios of inversion strength to surface flux and subjected to the same forcing, will not diverge rapidly. Nevertheless, understanding the capability of the ENKF to vertically spread screen-height information through the PBL within a simple framework is a necessary step toward more complex studies.

A "true" PBL state is randomly chosen from the climatology, and observations are sampled from the portion of the climatology trajectory beginning at this point. A total of 10 cases are randomly chosen to ensure that results do not depend on the particular initialization time. Ensembles of 50 members are generated for each case by randomly selecting additional PBL states from the climatology, and therefore the ensemble initialization and the subsequent observations are from the same distribution. The ensemble members are identically forced with the solar cycle parameterized according to the Julian day of the "truth" integration and run for 15 days. The domain is 120 layers spaced 100 m apart, and the time step is 60 s. An example of an initial ensemble selected from the climatological distribution is shown in Fig. 1.

Three parts to each experimental case are constructed around the ensembles. In the first (BASE), no assimilation is performed and the ensemble is allowed to evolve on its own. Second, the ENKF is applied hourly to assimilate layer-1 temperatures drawn from the "truth", to which observational noise is added. Observation error variance is set to the small value of 0.1 K. Third (FDDA), Newtonian relaxation is applied to assimilate layer-1 temperatures into every ensemble member independently. The nudging parameter is 1.0 at each hour (when the ENKF assimilation takes place), and falls along a Gaussian curve with a standard deviation of 7.5 minutes on either side of the assimilation time. Thus in

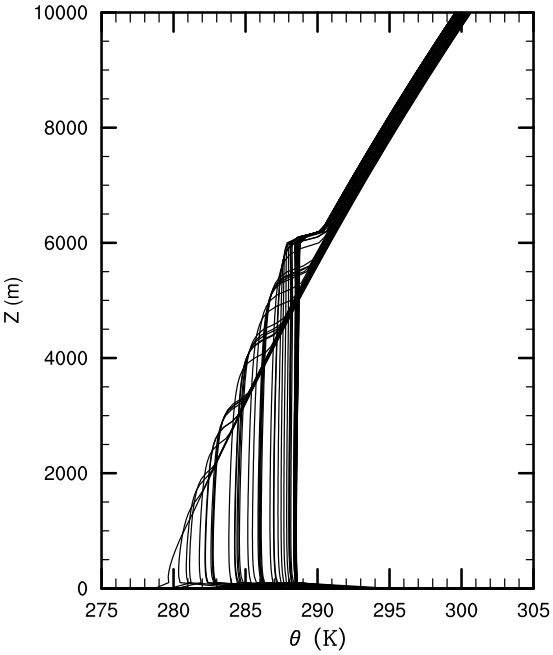

Figure 1: An example of potential temperature (θ) profiles randomly selected from the climatological distribution.

FDDA, the assimilation is perfect on the hour at the observation location, and the observations are considered perfect. In both cases, observations are assimilated beginning at time $t = t_0 + 5$ days, where t_0 is the randomly-chosen initialization time, and continuing to the end of the integration. By assimilating layer-1 temperatures rather than screen-height temperatures, complicated forward operators are avoided in this simple experiment.

3. Results and discussion

The reduction in ensemble spread (variance) is referred to as collapse, and comparing the spread and ensemble-mean error of ensembles ENKF and FDDA to those of BASE gives an estimate of the effectiveness of each assimilation system. With no assimilation, the identical solar forcing causes a slow collapse and slow error reduction. In the ENKF and FDDA ensembles, faster collapse and lower error may be attributed to the assimilation scheme. Observation error variance will prevent the complete collapse of the ENKF ensemble.

Figure 2 shows the slow collapse of the BASE ensemble for both the whole profile (top) and the skin temperature (bottom), and Fig. 3 shows the corresponding ensemble-mean error. This can be understood in the context of the linear nature of the model and the climatology. The warmest members of the ensemble represent one climatological extreme. When forced with solar radiation

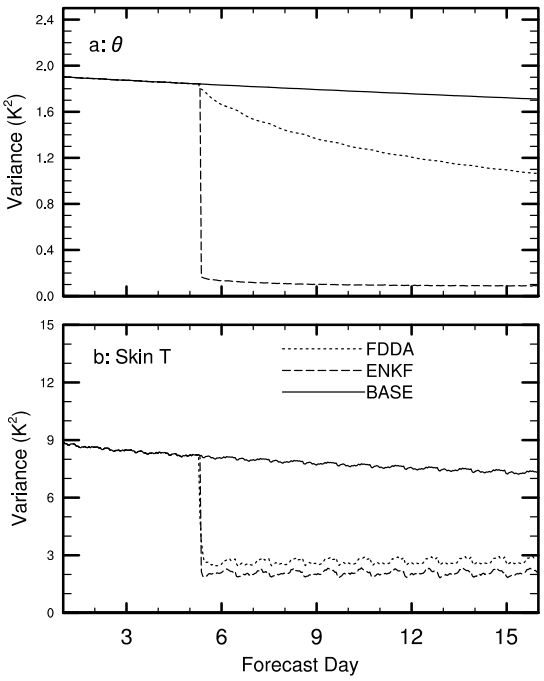

Figure 2: Ensemble variance for (a) the potential temperature (θ) profile, and (b) the skin temperature. Results are averaged over 10 cases.

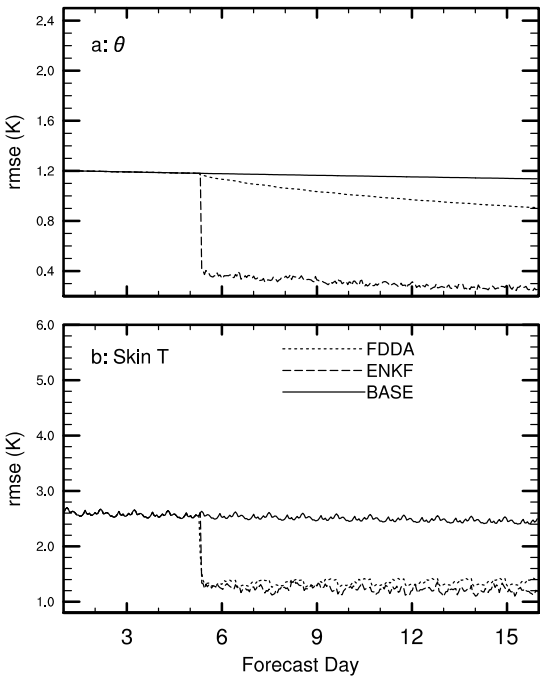

Figure 3: Ensemble mean rmse for (a) the potential temperature (θ) profile, and (b) the skin temperature. Results are averaged over 10 cases.

alone their states will not rapidly change. The system constrains the profile from further warming, and surface cooling leads to decoupling of the surface layer and the residual layer, leaving most of the profile intact. The cooler members of the ensemble approach the warmest members on a time scale proportional to the difference in time between the random states. Thus the BASE ensemble collapse and corresponding ensemble-mean error reduction is associated with the cooler states approaching the warmer states.

The immediate collapse of the ENKF ensemble and its error reduction are also apparent in Figs. 2 and 3. The finite value at which the variance and rmse settles is modulated by the assigned observation error variance. More observational error variance results in more persistent spread and higher rmse. Without nonlinear error growth the ensemble spread remains small through subsequent assimilation cycles. For example Fig. 4 shows one case of ensemble ENKF at noon local time on day 14 ($t = t_0 + 14.5$ days).

The collapse of the profiles and rmse reduction are only slightly faster in ensemble FDDA than BASE, but the skin temperature correction rivals the ENKF in effectiveness (Figs. 2 and 3). In the case that the layer-1 corrected temperature is cooler than the prior profile, the surface sensible heat flux rapidly increases and the skin temperature cools to approach the true skin temperature. The down-welling long-wave radiation also reduces with the lower temperature, causing the net long-wave radiative flux to tend upward and further cool the surface. Conversely, a warmer corrected layer-1 temperature will allow the skin to warm by reducing its heat loss via sensible heat flux and long-wave radiative flux, also tending to correct the skin temperature.

Although the layer-1 temperature and skin temperature are quickly corrected by the close connection between them, the upward spread of information relies on the solution to the diffusion equation. In the case when the skin temperature is warmed, information may propagate rapidly via PBL diffusion, but when the skin temperature is cooled no mechanism exists to transfer information vertically. Thus the profile collapse and ensemble-mean rmse reduction remain slow.

These results reflect the simplest application of nudging and do not include any bulk correction of the PBL state arising from prior knowledge of its behavior. Therefore they do not represent the best attempts at using relaxation techniques to assimilate screen-height observations (c.f. Stauffer et al. 1991; Miller and Benjamin 1992; Fast 1995; Ruggiero et al. 1996; Leidner et al. 2001). Conceivably, covariance estimates from the ensemble could be used to vertically spread the effect of the screen-height observations by nudging explicitly through the depth of covariance structures. The results should

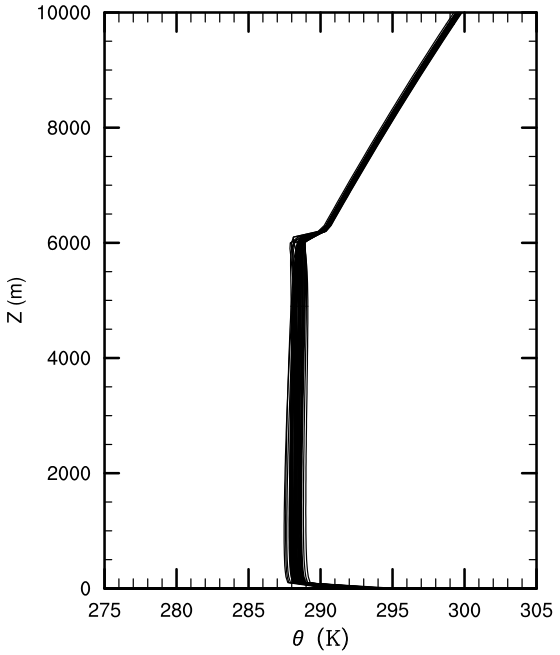

Figure 4: An example of potential temperature (θ) profiles for ensemble ENKF at time $t = t_0 + 14.5$ days.

be similar to the ENKF and may be superior to profile matching and bulk PBL adjustment because no ad-hoc assumptions about the structure near the top of the PBL are required. But in the ensemble framework, nudging is superfluous because the ensemble requires the filter update step to provide an estimated posterior distribution for re-initialization.

Because of the simplifications employed, this experiment does not include the full variability of the real PBL or of a PBL simulated by a complete NWP model. Specifically, these cases develop a mixed layer every day and retain correlation between the surface and the residual layer every night. External dynamics would tend to destroy the correlation between the surface and residual layer when they are decoupled under stable situations. In cases where destruction of the surface/residual layer correlation occurs on time scales shorter than the assimilation cycle, this approach may fail. But frequent updates (< 1 hr) are possible with mesonet data and external forcing would have to be strong to destroy the correlation completely.

These early results show the potential of the ENKF approach for using the assimilation of screen-height observations to correct the structure of an evolving PBL. Clearly, the problem only becomes more difficult as the the complexity of the dynamics increases. Because the development of the PBL is closely linked to lower boundary exchanges which may be poorly represented, model error is another real problem for any assimilation scheme dealing with PBL observations. Future work includes developing forward operators to relate the model state to the observations, and extending these results to 2- and 3-D cases within a complete NWP model. The DA cycle will also be used to estimate uncertain parameters in the model, thereby partially accounting for model error. Any results available will be presented.

REFERENCES

Anderson, J. L. and S. L. Anderson, 1999: A Monte Carlo implementation of the nonlinear filtering problem to produce ensemble assimilations and forecasts. *Mon.Wea.Rev.*, **127**, 2741–2758.

Deardorff, J. W., 1972: Parameterization of the boundary layer for use in general circulation models. *Mon.Wea.Rev.*, **100**, 93–106.

Fast, J. D., 1995: Mesoscale modeling and four-dimensional data assimilation in areas of highly-complex terrain. *J.Appl.Meteor.*, **34**, 2762–2782.

Hong, S.-Y. and H.-L. Pan, 1996: Nonlocal boundary layer vertical diffusion in a medium-range forecast model. *Mon.Wea.Rev.*, **124**, 2322–2339.

Leidner, S. M., D. R. Stauffer, and N. L. Seaman, 2001: Improving short-term numerical weather prediction in the California coastal sone by dynamic initialization of the marine boundary layer. *Mon.Wea.Rev.*, **129**, 275–293.

Miller, P. A. and S. G. Benjamin, 1992: A system for the hourly assimilation of surface observations in mountainous and flat terrain. *Mon.Wea.Rev.*, **120**, 2342–2359.

Ruggiero, F. H., K. D. Sashegyi, R. V. Madala, and S. Raman, 1996: The use of surface observations in four-dimensional data assimilation using a mesoscale model. *Mon.Wea.Rev.*, **124**, 1018–1033.

Stauffer, D. R., N. L. Seaman, and F. S. Binkowski, 1991: Use of four-dimensional data assimilation in a limited-area model part II: Effects of data assimilation within the planetary boundary layer. *Mon.Wea.Rev.*, **119**, 734–754.

Troen, I. and L. Mahrt, 1986: A simple model of the atmospheric boundary layer: Sensitivity to surface evaporation. *Bound. – LayerMeteor.*, **37**, 129–148.